Available online at www.sciencedirect.com
ScienceDirect
*Mendeleev Commun.*, 1996, **6(5)**, 203–205
Mendeleev Communications

# Influence of tunnelling on the ratio of the activation rate constants of C–C and C–H bonds in ethane by a bare palladium atom

**Victor M. Mamaev,* Igor P. Gloriozov, Andrew V. Prisyajnyuk and Yury A. Ustynyuk**

*Department of Chemistry, M. V. Lomonosov Moscow State University, 119899 Moscow, Russian Federation. Fax: + 7 095 932 8846; e-mail: vmam@nmr.chem.msu.su*

**Dynamic modeling of ethane oxidative insertion to a bare palladium atom at both C–C and C–H bonds has demonstrated the influence of quantum effects in the more growth of the rate constant of C–H bond activation compared to C–C activation.**

The development of mild and selective methods of alkane conversion to their functional derivatives by C–C and C–H bond breaking (*i.e.*, methods of alkane activation) is a fundamental chemical problem.[1] Oxidative addition of alkanes by bare transition metal atoms, clusters and their complexes[2] is known to be the most promising method of such activation.

Oxidative addition of ethane to a bare Pd atom can activate both the C–C and a C–H bonds:

In present, the potential-barrier heights ($V_{max}$) of both

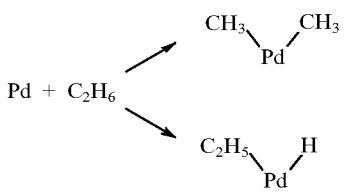


(1)

(2)

reaction (1)[3,4] and methane oxidative addition to a bare Pd atom [reaction (3)] are evaluated at an *ab initio* level.[3–5]

These results, as well as an orbital analysis,[6] may lead to the

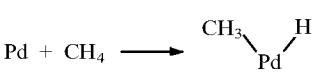


(3)

qualitative conclusion that the thermal rate constant of reaction (3) must be greater than that of reaction (1). However, for neither reaction (1) nor reaction (2), is there any mechanistic analysis at a level high enough to provide calculations of the thermal rate constants.

Earlier we developed a dynamic model of reaction (3) and showed tunnelling to contribute predominantly to the rate constant when $T < 200$ K.[7] Since one can presuppose *a priori*

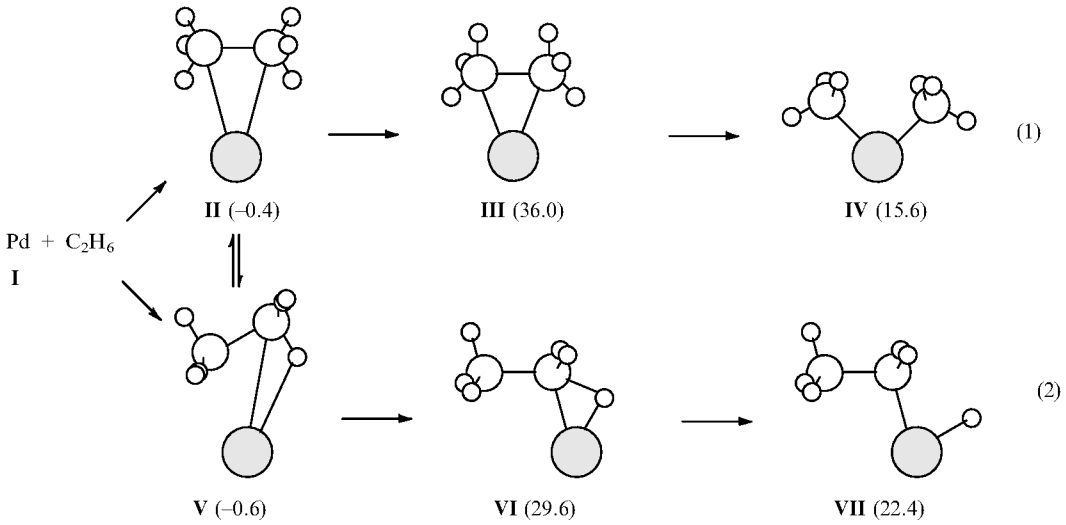


**Scheme 1**

that the tunnel contribution in the rate constant of reaction (2) must be much more than that of reaction (1) at any temperature, a question arises as to the influence of tunnelling on the thermal dependence of the ratio of the two constants ($k_2/k_1$).

We report here a detailed study of the mechanism of reactions (1) and (2) within the framework of the reaction-path Hamiltonian (RPH)[8] approximation. Such a study has made it possible to answer the question raised. For the construction of the RPHs we have employed a computer program[9] based on a semiempirical SCF CNDO/S[2] method.[10]

We have computed, using the software in ref. 9 the following RPH elements for both reactions (1) and (2):

- the $V_0(s)$ potential along the minimum-energy path (*i.e.*, reaction path), where $s$ is an intrinsic reaction coordinate expressed in terms of mass-weighted nuclear Cartesians.
- $\omega_i(s)$ frequencies of normal vibrations orthogonal to the reaction path.
- $B_{iF}$ functions of dynamic coupling between the motion along the reaction path and the transverse modes that determine the reaction path curvature (where $F = 3N-6 = 21$ is the number of degrees of freedom and $N$ is the number of atoms of the reactive molecular system).

The results of our calculations of the structures corresponding to the stationary points of the potential-energy surfaces (PESs) of reactions (1) and (3) agree with data obtained from the *ab initio* procedures with correlation and relativistic corrections.[3–5] As the reactive molecular system moves along a reaction path from the reactants toward the products, these structures appear in the sequence presented by Scheme 1 (where **II** and **V** denote precursor complexes, **III** and **VI** are transition states and **IV** and **VII** are reaction products. The values in parentheses are the energies of the PES stationary points in kcal mol$^{-1}$ with respect to the energy of the separated reactants).

The $V_0(s)$ potentials and the $\omega_i(s)$ functions that vary most markedly in the course of reactions (1) and (2) are depicted in Figures 1 and 2, respectively. We have determined that the motion along the former reaction path conserves one $C_2$ axis of the $D_{3d}$ point group of the ethane molecule. In addition, at point **IV** the system increases its point group from $C_2$ to $C_{2v}$. In the course of reaction (2) the system holds symmetry with respect to one of the $\sigma_d$-planes of the ethane molecule. These properties were used when Hessian matrices and the reaction path curvatures were being calculated.

The precursor complex **II** of reaction (1) lies at $s = -5.29$ A u$^{1/2}$. In this region, $\omega_i$ values are close to those of an intact ethane molecule, in particular, $\omega_3$ corresponds to

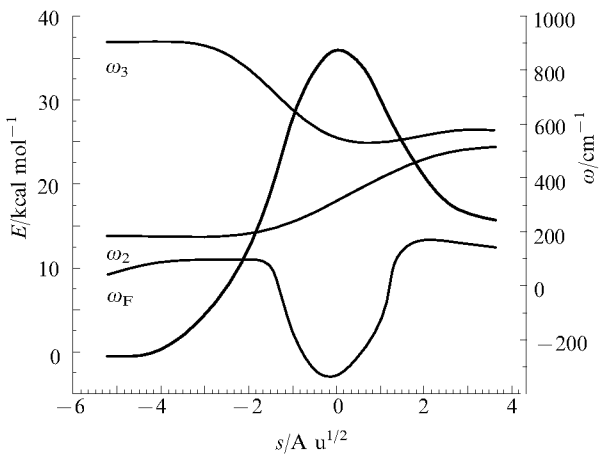


**Figure 1** Potential $V_0(s)$ along the path of reaction (1) and $\omega_i(s)$ frequencies that depend on $s$ most strongly.

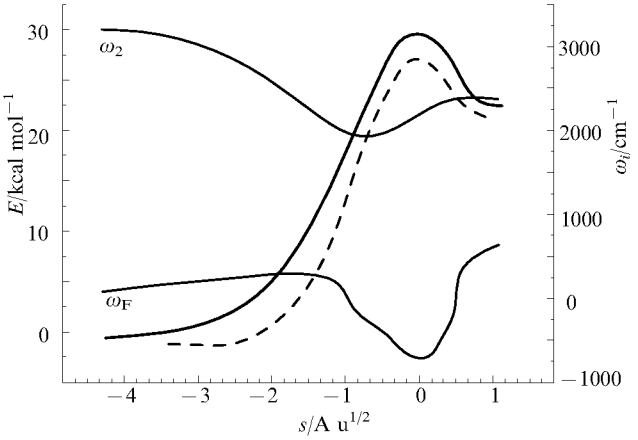


**Figure 2** Potential $V_0(s)$ along the path of reaction (2) (thick line) and $\omega_i(s)$ frequencies that depend on $s$ most strongly. $V_0(s)$ of reaction (3) (dashed line) is given for a comparison from ref. 7.

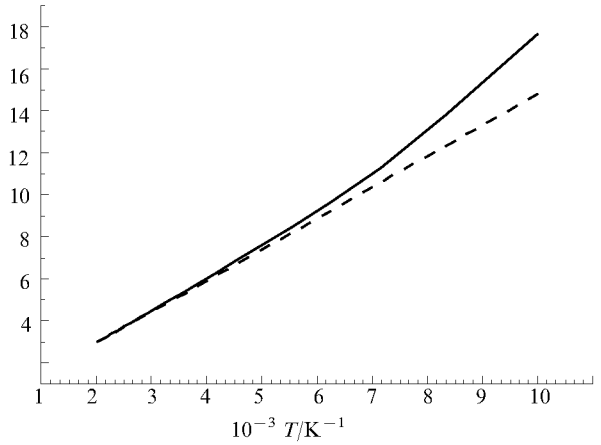


**Figure 3** Logarithms of the ratios of the cumulative (solid line) and the activation (dashed line) thermal rate constants of reactions (2) and (1) *versus* $T^{-1}$.

the ethane $Q$(C–C) vibration. Frequency $\omega_2$ becomes non-zero only when the Pd-ethane interaction has appeared. Near **IV** ($s = 3.56$ A $u^{1/2}$), $\omega_2$ and $\omega_3$ correspond to the $Q^-$(C–Pd) and $Q^+$(C–Pd) vibrations of $B_1$ and $A_1$ symmetry, respectively.

In the case of reaction (2) the totally symmetric $q$(C–H) ethane vibration with $\omega_2$ frequency (Figure 2) turns into the $q$(Pd–H) vibration of A′ symmetry.

An analysis of the shapes of the reaction path eigenvectors of reactions (1) and (2) in the basis of displacements of the internal coordinates revealed an analogy with the reaction path vector of reaction (3). In fact, in moving from a precursor complex to a transition state the variations of several internals contribute significantly to the reaction path: these are either $R_{Pd-C}$, $\gamma_{C-Pd-C}$ in the case of reaction (1), or $R_{Pd-C}$, $r_{Pd-H}$ and $\beta_{C-Pd-H}$ in the case of reaction (2). Conversely, in descent from a saddle point to a product only the $\gamma_{C-Pd-C}$ in the former case (or the $\beta_{C-Pd-H}$ in the latter case) bending deformation determines the reaction path eigenvector. Since along the latter reaction path section the distance between the Pd atom and the mass centre of the $CH_3$–$CH_3$ (or, respectively, $C_2H_5$–H) fragment changes little, the intrinsic normal reaction coordinate may well be substituted by a variation in $R_{C-C}$ (or $r_{C-H}$) with reasonable accuracy. On the other hand, these results show that a representation of the instrinsic reaction coordinate (IRC) by an individual geometry parameter would be wrong for the entire reaction path.

The reaction path of reaction (1) proved to be less curved than that of reaction (2). The first reaction path is most strongly coupled to $Q^+_{C-Pd}$ [$\omega_3$; $\max(B(s)_{3,F}) = 0.35\,A^{-1}\,u^{-1/2}$] mode, while the second one is afffected by $\beta_{CCH}$ [$\omega_5$; $\max(B(s)_{5,F}) = 0.85\,A^{-1}\,u^{-1/2}$], $Q_{PdC}$ [$\omega_2$; $\max(B(s)_{2,F}) = 0.64\,A^{-1}\,u^{-1/2}$] and $q_{PdH}$ [$\omega_{13}$; $\max(B(s)_{13,F}) = 0.68\,A^{-1}\,u^{-1/2}$] modes. For both reactions, the other $(B(s)_{i,F}) < 0.05\,A^{-1}\,u^{-1/2}$. The $B(s)_{i,F}$ functions for reaction (2) resemble those for reaction (3), which were computed in ref. 7. The cumulative reaction path curvature

$$\kappa = \left(\sum_{i=1}^{F-1} B_{iF}^2\right)^{1/2}$$

reaches $1.45\,A^{-1}\,u^{-1/2}$ for reaction (2) and $0.47\,A^{-1}\,u^{-1/2}$ for reaction (1).

The thermal rate constants $k(T)$ are calculated in terms of the quasi-classical approximation through the reaction probabilities $P(E)$, which depend on the translational energy of the reactants in their ground state.[7] The $P(E)$ values were evaluated using the vibrationally-adiabatic potential functions $V(s)$:

$$V(s) = V_0(s) + \sum_{j=1}^{3N-7} \left(\vec{n} + \frac{1}{2}\right) \frac{h\omega_j}{2\pi},$$

where $\vec{n}$ denotes the vector of vibrational quantum numbers.

From Figure 3, quantum effects have a greater affect on the reaction (2) mechanism compared to that of reaction (1). In particular, for reaction (2) the transmission factor (*i.e.*, the ratio of the cumulative rate constant to the Arrhenius one) exceeds 2 when the temperature falls below 180 K, whereas reaction (1) occurs mainly by the activation mechanism at any temperature. If one introduces the reaction path curvature into the expression for $P(E)$, the $k_2/k_1$ ratio will grow still further by either one order of magnitude at $T = 100$ K, or 10% at $T = 300$ K.

## References


1 A. E. Shilov, *The Activation of Saturated Hydrocarbons by Transition Metal Complexes*, Riedel, Dordrecht, 1984.
2 *Activation and Functionalization of Alkanes*, ed. L. Hill, Wiley, New York, 1989.
3 J. J. Low and W. A. Goddard III, *Organometallics*, 1986, **5**, 609.
4 M. A. Blomberg, P. E. M. Siegbahn, V. Nagashima and J. Wennerberg, *J. Am. Chem. Soc.*, 1991, **113**, 424.
5 M. A. Blomberg, P. E. M. Siegbahn and M. Svensson, *J. Am. Chem. Soc.*, 1992, **114**, 6095.
6 J. Y. Saillard and R. Hoffmann, *J. Am. Chem. Soc.*, 1984, **106**, 2006.
7 V. M. Mamaev, I. P. Gloriozov, S. Ya. Ishchenko, V. V. Simonyan, E. M. Myshakin, A. V. Prisyajnyuk and Yu. A. Ustynyuk, *J. Chem. Soc., Faraday Trans.*, 1995, **91**, 3779.
8 W. H. Miller, *J. Phys. Chem.*, 1983, **87**, 3811.
9 V. V. Rusanov, I. P. Gloriozov and V. M. Mamaev, *Zh. Strukt. Khim.*, 1993, **34**, 170 [*J. Struct. Chem.* (*Engl. Transl.*), 1993, **34**, 326].
10 M. J. Filatov, O. V. Gritsenko and G. M. Zhidomirov, *J. Mol. Catalysis*, 1989, **54**, 452.



*Received: Moscow, 28th March 1996*
*Cambridge, 3rd May 1996; Com. 6/02464E*